Atomic clusters and nanoscale particles: From coarse-grained dynamics to optimized annealing schedules

Ralph E. Kunz[a),b)]
Institut für Theoretische Physik, Technische Universität Berlin, Sekr. PN 7-1, Hardenbergstr. 36, D-10623 Berlin, Germany

Peter Blaudeck and Karl Heinz Hoffmann
Institut für Physik, Technische Universität Chemnitz-Zwickau, D-09107 Chemnitz, Germany

R. Stephen Berry
Department of Chemistry, The University of Chicago, Chicago, Illinois 60637

(Received 10 June 1997; accepted 30 October 1997)

An adaptive method is presented to optimize schedules for the simulated annealing of clusters and nanoscale particles. The method, based on both molecular-dynamics simulations and a set of master equations, is applied to a model configuration space for which the exact optimal schedule can also be found. The adaptive method is demonstrably suitable for optimizing larger and more realistic systems than can be treated by an exact method, even one based on a statistical-sample master equation. © *1998 American Institute of Physics.* [S0021-9606(98)50406-0]

I. INTRODUCTION

Annealing, carried out in simulation, has taken on an existence of its own as a means of solving optimization problems of many kinds.[1–3] Nonetheless, simulations of real annealing remain useful tools, particularly for studying the structures of clusters[4–13] and the dynamics of sintering.[14] Here, we combine the two aspects of simulations of annealing—formal optimization and modeling of real materials—to develop an optimization method for controlling the structures of clusters and nanoscale particles during their preparation. Two of the authors have recently demonstrated a way to explore and characterize topographies of potential surfaces in many dimensions, and to construct master equations to enable one to interpret flows of probability distributions or populations on those surfaces.[15–19] They have used a simple model to demonstrate the utility of the master equation for revealing the time scales for interbasin and intrabasin flows on complex surfaces,[17,18] thereby linking the knowledge of the forces between particles with the tendency of the system to form an amorphous structure or glass, or a ''focused'' structure such as a crystalline lattice, a Mackay icosahedron[20] or a specific folded structure such as that of a biologically active globular protein.[21]

In this paper we extend that investigation by introducing a controlled cooling procedure to optimize the final distribution of energies of clusters and nanoscale particles, and thereby, their distribution in configuration space. By this means, one controls the morphologies the clusters attain in their preparation. The concept of a controlled cooling procedure is of course in no way new. The novelty of this work is the manner in which that procedure is carried out, and its applicability to clusters and nanoscale structures.

Because the number of stationary points on multidimensional potential surfaces of clusters and nanoscale particles increases extremely rapidly with N, the number of particles in the particle, it is neither desirable nor possible to catalogue all these points for particles consisting of more than about 15 or possibly 20 atoms, ions, or molecules. Describing the topographies of such surfaces requires using statistical samples of the minima and saddles on the surface.[17–19] More precisely, the most useful distributions seem to be not those of the minima and saddles, but of the linked sequences of these stationary points specifically sequences that are monotonic in the energies of the minima, augmented by links between such sequences. A statistical sample of these sequences can be the basis of a viable statistical description of the probability flows on these complicated surfaces. A representative sample may be only a tiny subset of all the sequences on the cluster's potential surface, yet its size can still be considerable. For small enough clusters, numerical methods exist today that allow the determination of an optimal annealing schedule, i.e., to minimize the cluster's potential energy within a given time.[22] It is not feasible at this time to use those direct methods for larger systems such as nanoscale particles. Instead we must take recourse in adaptive methods to steer the cooling, methods which, because they are adaptive, use information from the structures and their thermal behavior.

The paper is organized as follows: In Sec. II we summarize how a coarse-grained description of a cluster's dynamics can be achieved by statistical means, i.e., how information from molecular-dynamics (MD) simulations can be used to construct a master equation to describe the cluster's dynamics. In Sec. III we describe the goals that annealing has the potential to achieve and introduce optimized and adaptive annealing procedures. In the subsequent section (Sec. IV) we apply these methods to a simplified Ar_{19} cluster, a system

a)Author to whom correspondence should be addressed. Present correspondence address: The Boston Consulting Group, Sendlingerstr. 7, D-80331 München, Germany, E-mail: kunz.ralph@bcg.com
b)R. E. Kunz has also published in this field under the surname Breitengraser-Kunz.

large enough to demonstrate the features of the different methods, yet small enough for the optimal annealing schedule to be computed directly from a statistical-sample master equation. Finally these results are discussed and summarized in Sec. V.

II. FROM MD-SIMULATIONS TO MASTER EQUATIONS: A COARSE-GRAINED DESCRIPTION OF CLUSTER DYNAMICS

The systems we consider here are clusters of atoms, molecules or ions—we use only examples of atomic clusters in this first work—whose dynamics can be well described by a single adiabatic potential surface. In contrast to small molecules, whose potential surfaces normally exhibit only one or perhaps a few stable geometries, clusters of atoms, molecules or ions, like condensed matter, may be found in any of a large number of locally stable geometric structures. The number of these structures grows extremely rapidly, probably at least exponentially, with N, the number of atoms or molecules in the system.[23,28] Clusters of more than about 15 atoms are so complex that we would not want to know all the minima and saddles on their potential surfaces, even if we had the computer time to find them. Useful knowledge of the potential surfaces for such clusters must come from a statistical analysis.

The convenient algorithms with which a sample of minima and saddles can be found on a given surface (cf. e.g., Ref. 30) make it possible to construct statistical databases of minimum-saddle-minimum (min-sad-min) sets, i.e., the configurations of two local minima linked by a single intervening saddle. If the analysis is carried out with sufficient energy resolution to avoid degeneracies among the minima (apart from permutational isomers), then each energy in the database that corresponds to a stationary point corresponds also to a unique geometry. It is straightforward to link the min-sad-min triples into *monotonic* sequences of stationary points, with the minima rising from low-energy points or ''basin bottoms'' on the potential surface.[15–18] Each of these low-energy points is the starting point for a set of monotonic sequences of minima; each set of these sequences defines a *basin* on the potential surface. The basins are separated by divides, like mountain passes. It is useful to call the basin containing the global minimum of the surface a *primary* basin and the corresponding monotonic sequences, *primary* monotonic sequences. The divide or saddle separating monotonic sequences leading to different minima is, according to this definition, the barrier that separates two adjacent basins. (It may be desirable at a later date to refine this definition, to use the highest saddle on the reaction path, rather than the monotonic sequences to define basins, in keeping with the common way to think of mountain passes.)

It is useful in some situations, particularly with larger systems, to use the name ''primary basin'' for other basins with the same kind of structure at their minima, for example in cases in which structure type and not absolute minimality is the important consideration. Such a broader definition would be appropriate in comparing icosahedral and close-packed van der Waals cluster of thousands of atoms, for which the transition between the two structure types is a dominant question. Obviously basins separated by one divide from a primary basin are secondary basins, and so on.

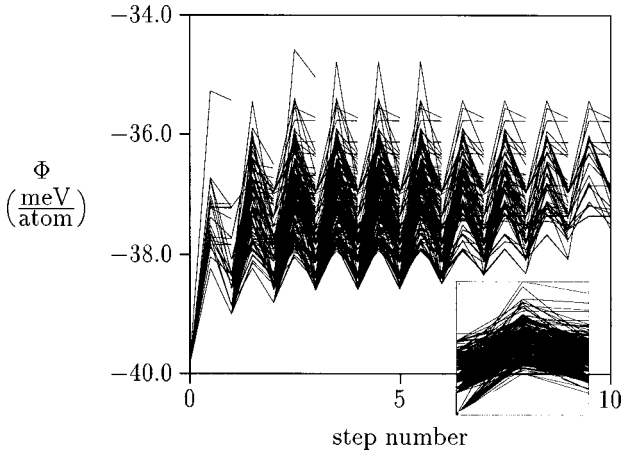

FIG. 1. Primary monotonic sequences in the sample database for Lennard-Jones 19-particle cluster; inset: All minimum-saddle-minimum triples in the database.

This categorization of the surface into basins with wells within them allows us to study dynamics on the surface without treating explicitly the rapid intrawell vibrations. Instead, by using transition state theory in any of its forms, we average over these high-frequency modes and concentrate on the interwell and interbasin transition. The rates for these transitions may be computed in a variety of ways,[24] depending on whether one wishes to describe the system classically or quantum mechanically, and on the desired level of accuracy and sophistication. Passages among the minima on the potential surface of alkali halide tetramers and pentamers seem to be reliably described by the RRKM (Rice–Ramsperger–Kassel–Marcus) model with anharmonic vibrations;[25] larger clusters, notably Ar_{55} and $(KCl)_{32}$ also thermalize as they relax configurationally and move isothermally down monotonic sequences.[29] This means that each rate coefficient can be determined reliably from the partition functions for the initial minimum and the appropriate connecting saddle. Here, as in other models in which intrawell vibrational equilibration to a bath temperature T is fast compared with interwell equilibration, the matrix $\underline{k}$ of temperature-dependent transition rate coefficients $k_{i,j}$ for passage between all the adjacent pairs (i,j) of local minima in the statistical data base depends parametrically on T.

(Breitengraser-)Kunz and Berry[15–18] analyzed a 19-particle Lennard-Jones system, to investigate this approach. The configuration space of that system is so large that one must use a statistical sample of the minima and saddles of the potential surface instead of the complete (but unknown) set of its stationary points. In this case the sample consisted of 291 geometrically different minima $i=1,...,n=291$ ordered with rising energy $\Phi_i<\Phi_{i+1}$, and 461 saddles, each connecting a pair of minima in the database. The corresponding min-sad-min connections are shown in the inset of Fig. 1. Thus the reduced state space for this system can be described by an undirected graph whose nodes represent the minima; each edge represents a connecting saddle (and, implicitly, the lowest-energy path connecting the three stationary points). A

graphic realization of this state space, restricted to the monotonic sequences rising from the global minimum (*primary monotonic sequences*), is shown in Fig. 1. This surface has high barriers between all minima on the sequences, even those at low energy; almost all of these minima show no regularity in their structures. The result is that Ar_{19} has a potential surface with a sawtooth topography which makes the cluster tend strongly to take on amorphous structures when the clusters cool from their liquid state. Such a sawtooth topography makes annealing to the global minimum structure a difficult task. This is in sharp contrast to topographies found e.g., for $(KCl)_{32}$, which resemble staircases.[18,19] Staircase potentials guide and focus relaxation processes and facilitate annealing to highly selective, low-energy structures.

The relaxation of arbitrary initial population distributions on the surface emerges naturally from the master equation, in terms of its eigenvectors and eigenfunctions, which constitute ''eigenflows'' and their relaxation times. The master equation itself is the linear differential (matrix) equation whose nonvanishing coefficients are the rate coefficients $k_{i,j}(T)$, the inverses of the characteristic times $\tau_{i,j}(T)$, for passage between linked local minima i and j. An Einstein model was used by Kunz and Berry for the vibrational frequencies in the partition function, which corresponds to choosing the same characteristic time for all transitions. The same model is used here.

With the coefficients $k_{i,j}(T)$ in hand, we can construct the master equation for flows of populations on the surface at any desired temperature. Using an explicit Euler-forward time discretization, the discrete time dynamics of the probability $P(t_k) \equiv [P_1(t_k), P_2(t_k), \ldots, P_n(t_k)]^T$ is then given by

$$\underline{P}(t_{k+1}) = \underline{\underline{w}}(T(t_k))\underline{P}(t_k), \tag{1}$$

where $P_i(t_k)$ denotes the probability that the cluster be in minimum i at time t_k. Here n is the number of minima and we have defined $\underline{\underline{w}}$ by $w_{ij} \equiv \Delta t k_{ij} + \delta_{ij}(1 - \Delta t \Sigma_l k_{lj})$, with the given time step Δt, to simplify the notation.

Now we outline the subsequent development of this approach. We begin with the observation stated previously that each energy of a local minimum corresponds to a unique geometric structure (apart from permutational isomers). Hence each population distribution over the energies of the clusters corresponds to a distinct distribution of geometries. For atomic clusters with central interparticle forces and binary ionic clusters with Coulomb long-range forces and exponential short-range repulsions, these can range from distributions in which most of the probability distribution is concentrated in the crystal-like or polyhedral ground state to high-energy distributions in which amorphous, irregular states are favored. Which morphology a cluster exhibits depends on the topography of the potential and the temperature schedule in which its structure evolved. Some systems, such as the rare-gas clusters, fall readily into minima corresponding to amorphous structures, and have thus been identified as ''glass-formers,'' while others, such as alkali halide clusters, go readily to specific structures, rocksalt crystallites in this example, and have therefore been called ''structure seekers.''[19] Hence, by choosing annealing schedules suitable to the particular system, we can manipulate the ensemble of final structures we are likely to find. Ways to do this will be explored in the following section.

To imagine the state space structure in which we wish to describe the transport of probability, the reader should consider the energy function as a high-dimensional surface with hills and valleys, for which we know the locations (coordinates) and attitudes (energies) of the bottoms of those valleys and of the saddles that allow passage between all of these valleys, and the curvatures—force constants—of the surfaces at all the stationary points. It is possible to determine anharmonicities as well, but the treatment here neglects these and even, by its use of an Einstein model for vibrations, neglects the variations of force constants. The problem of the accuracy of the rate coefficients in the master equation is treated elsewhere[31]

III. ANNEALING: AN EFFICIENT MEANS OF STRUCTURE SELECTION

We can now begin a simulated annealing process by postulating an isothermal distribution, such as a random Boltzmann distribution among the individual wells, which one might find in a hot, liquid cluster. (Ideally, this distribution could best be constructed if we knew the microcanonical entropies of all the wells at all energies, in effect the $3N$-6-dimensional areas of all the lakes in the space of $3N$-5-dimensions, including the energy as one of the dimensions.) Then we can cool the distribution in a simulation, letting the master equation describe how the distribution relaxes from the higher initial temperature as it approaches the lower second temperature. We have proposed three different criteria for the fixing the durations of the intervals at each successive, lower temperature and implemented two of these in the examples below. The programs considered here make only monotonic temperature changes; no reheating occurs in these optimizations.

One can then set a final-state target, which may be just a minimum mean final potential energy or may be a specific population distribution, e.g., to correspond to a desired morphology or distribution of morphologies in the product particles. In the latter case, one needs a criterion of success in approaching that target. Let us call that target distribution D_i. The simplest examples would be: (a) Attainment of the global minimum, for which $D_i = \delta_{i,1}$, and (b) attainment of a random distribution dominated by amorphous structures, i.e., a glass, for which, in a complex system with n local minima, most of which correspond to amorphous structures, one could set $D_i = 1/n$. In less obvious cases, one might seek a desired mix of amorphous character, perhaps for electrical properties, and crystalline or polyhedral character, for structural strength or for matching the structure of a substrate. The most direct approach sets a prior schedule for the temperature and follows that. An alternative and more sophisticated approach to obtain the desired final structure includes feedback: One may use the form of the evolving cooling distribution to guide the temperature program and thereby exert a degree of control on the structures as the system follows the master equation at successively lower temperatures. We will introduce such adaptive methods in part B of

this section. However it is feasible to carry out the first kind of explicit optimization of the temperature schedule for small systems and specific desired final structures. A brief description of such a procedure is given in Sec. III A.

A. Explicit optimization

This optimization is carried out by determining that schedule which leads the ensemble of clusters to the minimum of the mean final potential energy

$$\langle \Phi \rangle_M = \sum_{i=1}^{n} \Phi_i P_i(t_M), \tag{2}$$

where M is the number of time steps available, one of the constraints of the optimization. In all cases the initial probability distribution $\underline{P}(0)$ was taken to be the equilibrium distribution at $T=400$ K, a temperature at which this model system is fluid. This, together with the fixed cluster size (mass conservation) and force law, constitute the other constraints. The final probability distribution $\underline{P}(t_M)$ is determined from

$$\underline{P}(t_M) = \prod_{k=0}^{M-1} \underline{\underline{w}}[T_{\mathrm{opt}}(t_k)]\underline{P}(0). \tag{3}$$

The optimal schedule $T_{\mathrm{opt}}(t_k)$ is computed by an iterative algorithm based on control theory.[26,27] The algorithm relies on successive modifications of an initial annealing function and calculates the probability distributions at each time step starting from an initial distribution.

Essentially the function $\langle \Phi \rangle_M$ has to be minimized as a function of the variables $T(t_k)$, where $\langle \Phi \rangle_M$ depends on the $T(t_k)$ through the final distribution $\underline{P}(t_M)$. This minimization must be performed under the constraints of Eq. (3). This leads to the minimization of the functional

$$F = \langle \Phi \rangle_M + \sum_{k=0}^{M-1} \underline{\Lambda}^T(t_{k+1})(\underline{\underline{w}}(T(t_k))\underline{P}(t_k) - \underline{P}(t_{k+1})), \tag{4}$$

where $\underline{\Lambda}^T(t_k)$ are Lagrange parameters. Then the usual variational principles are used. For a more detailed description see Ref. 26.

The computations converge rapidly, within hours even for $n=291$ states with the particular workstation we used, so the process can be considered practical. The precise computation time is not particularly relevant, but it is relevant that one can expect to treat considerably larger systems as the algorithms and computers become more efficient.

B. Adaptive annealing procedures

The motivation for using either explicit optimization or adaptive annealing procedures is to simulate scheduled cooling of a distribution in a simulation, letting the master equation describe how the distribution from a higher temperature T relaxes as it approaches a lower second temperature $T-\Delta T$. A ''thermostat'' built into the simulation will then decide when the system temperature should be reduced by another fixed increment ΔT. Systems of many particles are too complicated to be treated by explicit optimization.

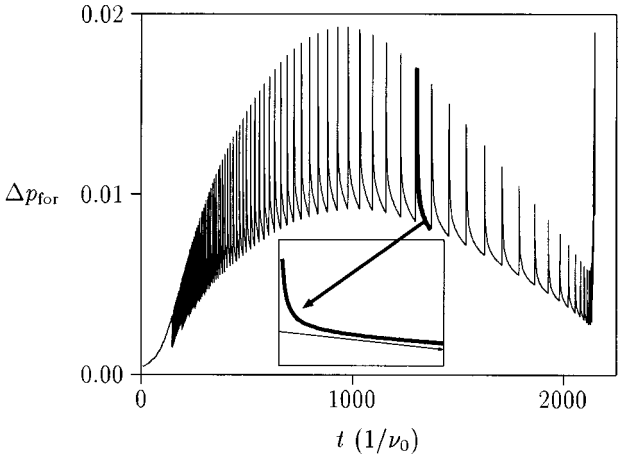

FIG. 2. The fraction of downward moves to all moves, $\Delta p_{\mathrm{for}} \equiv p_{\mathrm{for}} - 1/2$ as a function of time for $\beta=0.75$ and method 2: The system's temperature is lowered at time t_i by ΔT, as soon as $\ln[\Delta p_{\mathrm{for}}(t_i)/\Delta p_{\mathrm{for}}(t_{i-1})] \leqslant -\beta$ holds. Inset: Logarithm of Δp_{for} vs time for one switching period; after a transient period the decay is approximately exponential.

For increasing system size, i.e., increasing N, the number of constituents of the clusters or nanoscale particles, the complexity of the corresponding multidimensional potential surfaces increases very rapidly. Along with this probably hyperexponential growth of the number of minima on the surface,[23,28] the number of minima in any representative sample of min-sad-min triples rises, significantly increasing the dimension of the probability density $\underline{P}$. While we might, with very large efficient computers, use the explicit procedure described above for clusters of tens or even hundreds of particles, we could not possibly use such a method for nanoscale materials. To deal with larger particles, we turn to adaptive annealing methods.

To define a thermostat, we found it useful to construct a functional of probability space, namely the fraction p_{for} of the well-to-well transition processes that are energy lowering; this is defined as $p_{\mathrm{for}} \equiv \Sigma_i \Sigma_{j<i} k_{j,i} P_i / \Sigma_i \Sigma_{j \neq i} k_{j,i} P_i$ with the order of indices the same as the order of energies. Its deviation from 0.5 determines the ''distance'' from the stationary or quasi-stationary distribution at the respective temperature, i.e., one whose largest eigenvalue lies so close to zero that the corresponding eigenstate is in practice indistinguishable from an equilibrium state.

We chose two patterns of thermostats, based on the functional p_{for}. In the first (''method 1'') the temperature was incrementally reduced when $\Delta p_{\mathrm{for}} \equiv p_{\mathrm{for}} - 0.5$ fell below a given fixed threshold α. In the second (''method 2''), the temperature was reduced when the ratio of the current value of Δp_{for} to the value of Δp_{for} at the last temperature change fell below $e^{-\beta}$. This means that if the decrease occurred exponentially, switching of the temperature would occur after the fraction of the decay time $\tilde{\tau}$ given by $\beta\tilde{\tau}$. The inset of Fig. 2 shows that the decay is approximately exponential after some transition time.

We could shift the distribution of occupation of the system's minima in such a way that the mean potential energy took on virtually any desired value between the extreme cases obtained by instant quenching ($\beta=0$) and by quasistatic cooling ($\beta \to \infty$). The results are given in Sec. IV. The

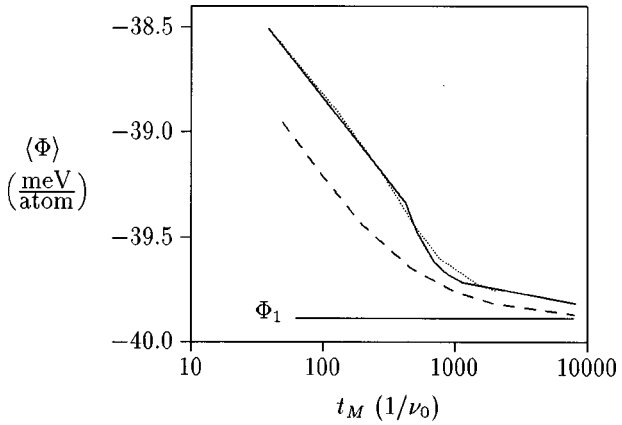

FIG. 3. Final mean potential energy after annealing, $\langle\Phi\rangle_M$, as a function of the annealing time t_M for method 1 (solid), method 2 (dotted), and optimal schedule (dashed).

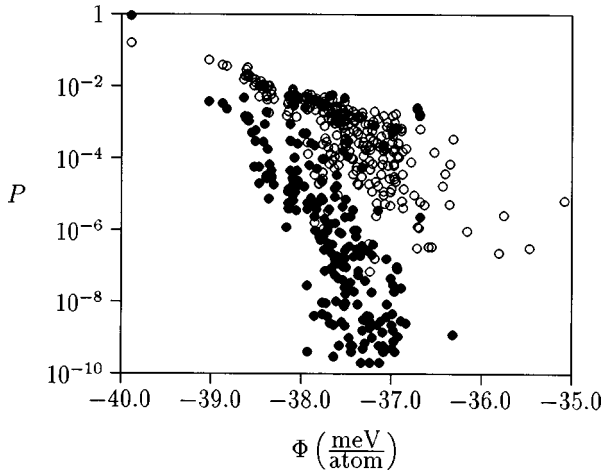

FIG. 4. The probability distribution $P(\Phi_i)$, $i=1,...,n$, after annealing according to different schedules of method 2: $\beta=0$ (circles), $\beta=0.75$ (bullets).

Euler-forward algorithm we used for the iteration of the master equation allowed computation times of several seconds to a minute for one run (depending on the number of time steps).

IV. ANNEALING RESULTS FOR A MODEL CLUSTER

The model system used here is based on the 19-atom cluster particles bound by Lennard-Jones pairwise potentials, the same system used in the previous analyses.[15–18] We made several assumptions in that work in order to simplify the initial exploration of the method, so we must be very cautious about identifying the model system with real clusters of argon, for example. The rate coefficient matrix was computed within an Einstein model for the wells, assuming that they all have the same spectra of intrawell vibrations with the single frequency ν_0. (In the following we use the inverted frequency $1/\nu_0$ as the time unit), This means that the transition matrix is highly simplified by comparison with a real, statistically based sample matrix. However all the adjacencies of the database for the 19-atom L-J (Lennard-Jones) cluster were retained.

One issue pointed out previously[17] is the question of the robustness of the statistical sample. At present, this is an open question; a proper test will be comparison of sets of sequences determined from altogether independent sets of searches, to establish their similarity, or comparison of a set of sequences with another set of twice as many. Points that will require particular attention are the definition of ''similarity'' of sequences, and the robustness of the sample with respect to links between sequences. To date, the only tests of robustness we have carried out establish that the distributions of the energies of minima and saddle points for these clusters are well replicated by independent searches.

We performed a number of computer runs (with time steps of $0.1/\nu_0$), using both method 1 and method 2 with various parameters α and β, resulting in various annealing schedules $T(t_i)$, $i=1,...,M$ and times t_M. In Fig. 3 the mean final energies $\langle\Phi\rangle_M$ of these schedules are given in terms of the annealing time τ_M. Additionally we show the results of the optimal annealing schedules obtained for the same annealing time τ_M. Due to the given time step of $\Delta t=0.1/\nu_0$ and temperature increment of $\Delta T=1$ K, the minimum annealing time of the adaptive method was $\tau_M=39/\nu_0$ for annealing from $T_1=400$ K to $T_{390}=10$ K. Successively increasing the annealing time τ_M, we see that the cluster passes from high-energy structures with mean energy $\langle\Phi\rangle_M=-38.5$ meV/Atom to approach the global minimum structure with $\langle\Phi\rangle_M=\Phi_1=-39.8864$ meV/Atom. Based on the actual annealing time τ_M, any mean energy $\langle\Phi\rangle_M$ between these two extremes can be reached. Comparing the adaptive methods with the optimal, we see that with increasing t_M the adaptive schedules better approximate the final energy of the optimal schedule. The differences in the final energy are relatively small for schedules with annealing times longer than about $400/\nu_0$ corresponding to more than 4000 computer time steps. Consequently, any disadvantages of an adaptive schedule, necessary in order to handle large, complex systems, seem to decrease with increasing annealing time. It will later be suggested that an adequate choice of the time step Δt used in the simulation is the major level for narrowing this gap.

To illustrate the effect of different annealing times on the final state of the system, in Fig. 4 we have plotted the distributions $P_i=P(\Phi_i)$, $i=1,...,n$ of the probabilities for two examples of method 2: $\beta=0$ and $\beta=0.75$ corresponding to $t_M=39/\nu_0$ and $t_M=2100/\nu_0$, respectively. The slower the annealing procedure is performed, the greater the degree to which the higher energy levels surrender probability to the ground state. In this case successive temperature decreases take place faster than the configurational equilibrium between the higher-energy wells and lower energy wells can drive the probability density downhill. This is a quenching process at a finite rate. Due to the rapidly decreasing temperature, the high barriers of Ar_{19} (cf. Fig. 1) trap the system in the higher-lying wells. As opposed to alkali halides such as $(KCl)_{32}$, where many of the downstream barriers are lower than the drops in energy from one minimum to the next, and the primary monotonic sequences resemble a staircase,[18,19] the sawtooth topography of Ar_{19} requires ex-

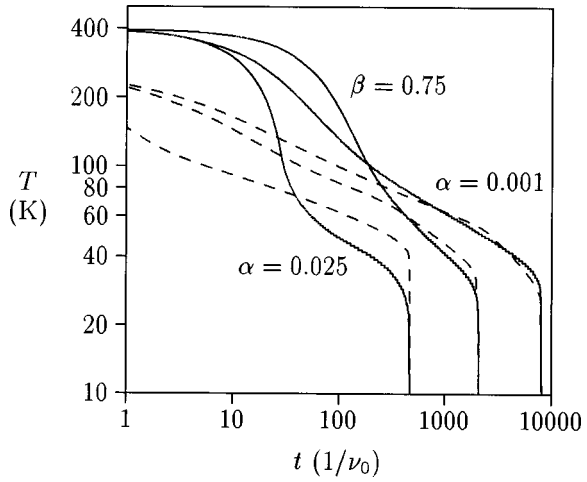

FIG. 5. Annealing schedules for different values of α (Method 1) and β (Method 2) (solid curves) and the corresponding optimal annealing schedules (dashed curves).

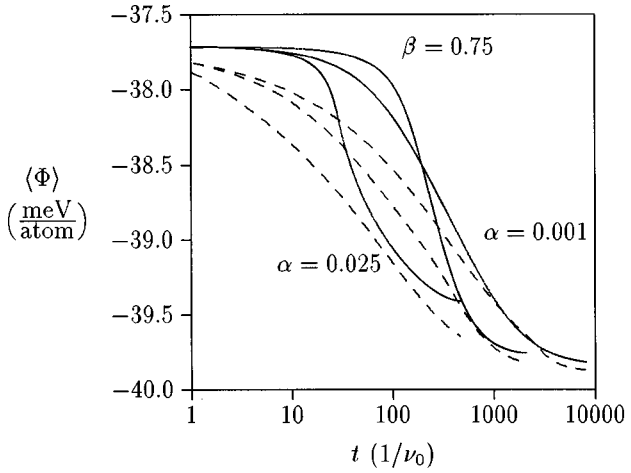

FIG. 6. Mean potential energy $\langle\Phi\rangle$ as a function of time t for the adaptive annealing schedules (solid curves) of Fig. 5 and the corresponding optimal schedules (dashed curves).

tremely slow annealing to reach a low-energy morphology such as the one denoted by the bullets in Fig. 4: 95% of the probability density is accumulated in the ground state. (It should be noted again that in the simulated annealing for $\beta=0$, (from $T_1=400$ K to $T_M=10$ K), t_M could not approach 0 but was $t_M=39$ instead, since the temperature T_i could not be lowered quicker than the simulation time step of $0.1/\nu_0$.)

In Fig. 5 we have explicitly plotted the annealing schedules $T(t_i)$, $i=1,...,M$ for three values of the parameter of the adaptive methods ($\alpha=0.025$, $\alpha=0.001$, $\beta=0.75$) and for the corresponding optimal method. In all cases the optimal schedule requires a particularly small cooling rate in the range 100–50 K. The adaptive schedules require their slowest cooling in a somewhat different range of about 80–30 K. The slow decrease of the temperature for the first time steps is simply an effect caused by the artificially limited cooling rate that persists in all adaptive schedules. At the beginning of the annealing procedure, the optimal allowed cooling rate may be determined by the boundary of the allowed range of such rates; this can give rise to overly rapid cooling rates in particular temperature ranges at later time.

Finally in Fig. 6, plots of the resulting mean potential energy vs time, $\langle\Phi\rangle(t)$, are shown for the examples given in Fig. 5. The curves reflect the effect of the corresponding temperature functions $T(t)$. We see that their limited cooling rates in the initial phase of the simulations make the adaptive schedules slower than the optimal method to reduce the mean energy. It may be possible to overcome these limitations by using more judicious time steps Δt; this is under study now. Particularly, it seems possible to decrease the gap in efficiency between the adaptive and optimal methods apparent in Fig. 3. Note that the differences in the final energies are already part of the data in Fig. 3.

In this early stage of the development of the method, to keep the calculations simple and transparent, we have deliberately used an oversimplified model rather than an accurate representation of an actual cluster. However, since the steps for further refinement are well known, we plan to carry the computation to a more realistic system, with realistic force constants and anharmonicities in the next stage of the work.[31]

V. DISCUSSION

The methods introduced here to obtain annealing schedules are based on the master equation dynamics of a system's probability distribution, which determine the probability of finding the system within the catchment basin of each well of the potential surface of the system at any chosen time. Given a system with Markovian kinetics and (hypothetical) exact knowledge of the transition matrix, the temporal evolution of this probability distribution is statistically equivalent to an infinite number of MD simulation runs. Thus, if we have a way to compute the transition coefficients reliably, and the statistical database of stationary points is robust, the master equation approach gives us an extremely compact description of the dynamics of a system evolving in its configuration space. Additionally, this compact description allows us to check the influence of changes in external parameters, the easiest being the system's temperature, in a way far more efficient than by MD simulations. If we wish to use MD simulations to evaluate the impact of a single given cooling schedule, this schedule must be simulated with an adequately large ensemble of initial states. Using such a method to select a specific function $T(t)$ as the appropriate cooling schedule to optimize a specific objective, e.g., to minimize the system's potential energy, is extremely time consuming, if it is possible to do it reliably at all. On the other hand, the compact master equation description, with its smoothing and averaging over high-frequency intrawell modes, allows us to find adaptive methods, and for certain annealing goals like minimum potential energy, even optimal methods to determine these functions.

The computational effort becomes unreasonably high for any known optimization method for sufficiently large systems. However, where optimal methods exist and are feasible to use, they can not only be valuable per se; they can

also be used to determine the quality of adaptive methods as demonstrated above. On the other hand, the adaptive methods are applicable to much larger systems due to their computational simplicity, and are thus a promising tool for structure selecting processes.

It should be pointed out that the above method is not restricted to clusters and nanoscale particles but can also be applied to proteins and other polymers. The staircase topography of the basins on the $(KCl)_{32}$ potential surface described by Refs. 18 and 19, for instance, is similar to the kind of landscape that has been proposed recently for the potential surface of proteins.[21] Work using the method to examine proteins is under way.

In this paper we have presented a method to use coarse-grained configuration space dynamics of clusters and nanoscale particles to arrive at optimized annealing schedules or approximations thereof. In a next step, the simplified model system we used here must be extended to describe more realistically an actual atomic cluster, especially by computing the transition rate coefficients and increasing the size of the database. Also additional adaptive schemes must be found to anneal a system not only to the primary basin, but also to the structures within higher-order basins.

ACKNOWLEDGMENTS

We would like to thank T. Astakhova for generating the database of minima and saddles for the 19-atom Lennard-Jones cluster and P. Sibani, P. Wolynes, and R. Klages for stimulating discussions. R.E.K. acknowledges the financial support of the Institute of Theoretical Physics of the TU Berlin. R.S.B. would like to acknowledge the support of the National Science Foundation and the Alexander von Humboldt-Stiftung and K. H. H. acknowledges the financial support of the Deutsche Forschungsgemeinschaft. We would also like to thank the Telluride Summer Research Center for its hospitality in providing a setting in which this work could be carried out with suitable visual stimuli.

[1] S. Kirkpatrick, C. D. Gelatt, and M. P. Vecchi, Science **220**, 671 (1983).
[2] F. H. Stillinger and D. K. Stillinger, J. Chem. Phys. **93**, 6106 (1990).
[3] X.-Y. Chang and R. S. Berry, J. Chem. Phys. **97**, 3573 (1992).
[4] W. Andreoni, in *The Chemical Physics of Atomic and Molecular Clusters*, edited by G. Scoles (North-Holland, Amsterdam, 1990), p. 159.
[5] R. L. Asher, D. A. Micha, and P. J. Brucat, J. Chem. Phys. **96**, 7683 (1992).
[6] G. v. Helden, N. G. Gotts, and M. T. Bowers, J. Am. Chem. Soc. **115**, 4363 (1993).
[7] J. Hunter, J. Fye, and M. F. Jarrold, Science **260**, 784 (1993).
[8] J. M. Hunter, J. L. Fye, and M. F. Jarrold, J. Chem. Phys. **99**, 1785 (1993).
[9] M. F. Jarrold and J. E. Bower, J. Chem. Phys. **98**, 2399 (1993).
[10] R. O. Jones and G. Seifert, J. Chem. Phys. **96**, 7564 (1992).
[11] R. O. Jones, J. Chem. Phys. **99**, 1194 (1993).
[12] U. Nagashima, H. Tanaka, and K. Morokuma, J. Phys. Chem. **96**, 4294 (1992).
[13] M. S. Stave and A. dePristo, J. Chem. Phys. **97**, 3386 (1992).
[14] J. Bernholc, P. Salamon, and R. S. Berry, in *The Physics and Chemistry of Small Clusters*, edited by P. Jena, S. N. Khanna, and B. K. Rao (Plenum, New York, 1987), p. 185.
[15] R. E. Kunz, T. Astakhova, and R. S. Berry, Surf. Rev. Lett. **3**, 307 (1996).
[16] R. S. Berry and R. Breitengraser-Kunz, Phys. Rev. Lett. **74**, 3951 (1995).
[17] R. E. Kunz and R. S. Berry, J. Chem. Phys. **103**, 1904 (1995).
[18] R. E. Kunz, *The Dynamics of First-Order Phase Transitions. In Mesoscopic and Macroscopic Equilibrium and Nonequilibrium Systems* (Harri Deutsch, Frankfurt/M, 1995).
[19] K. D. Ball, R. S. Berry, R. E. Kunz, F.-Y. Li, A. Proykova, and D. J. Wales, Science **271**, 963 (1996).
[20] A. L. Mackay, Acta Crystallogr. **15**, 916 (1962).
[21] T. D. Bryngelson, J. N. Onuchic, N. D. Socci, and P. G. Wolynes, Proteins **21**, 167 (1995); P. G. Wolynes, J. N. Onuchic, and D. Thirumalai, Science **267**, 1619 (1995).
[22] R. S. Berry, Chem. Rev. **93**, 2379 (1993).
[23] C. J. Tsai and K. D. Jordan, J. Phys. Chem. **97**, 11227 (1993).
[24] P. J. Robinson and K. A. Holbrook, *Unimolecular Reactions* (Wiley-Interscience, London, 1972).
[25] J. P. Rose and R. S. Berry, J. Chem. Phys. **96**, 517 (1992).
[26] V. F. Krotov, Control Cybernetics **17**, 115 (1988)
[27] K. Ergenzinger, Thesis, University Heidelberg, 1993.
[28] R. S. Berry, K. D. Ball, H. Davis, F.-Y. Li, R. E. Kunz, A. Proykova, and D. J. Wales, Proc. 39th Conf. on Chemical Research of the Robert A. Welch Foundation, Houston, Texas 1996, p. 71.
[29] B. Vekhter, K. D. Ball, J. Rose, and R. S. Berry, J. Chem. Phys. 1 bf **106**, 4644 (1997).
[30] R. J. Hinde and R. S. Berry, J. Chem. Phys. **99**, 2942 (1993).
[31] K. D. Ball and R. S. Berry (in preparation).